Journal of Physics: Conference Series

PAPER • OPEN ACCESS

Sliding TLCD for vibration control of base-isolation systems: experimental comparison with traditional TLCD and TMD

To cite this article: C Masnata *et al* 2024 *J. Phys.: Conf. Ser.* **2647** 172005

Journal of Physics: Conference Series **2647** (2024) 172005 doi:10.1088/1742-6596/2647/17/172005

Sliding TLCD for vibration control of base-isolation systems: experimental comparison with traditional TLCD and TMD

C Masnata[1], A Di Matteo[1], C Adam[2] and A Pirrotta[1]

[1]University of Palermo, Department of Engineering, viale delle Scienze, 90128 Palermo, Italy
[2]Universität Innsbruck, Unit of Applied Mechanics, Technikerstr. 13, 6020 Innsbruck, Austria

chiara.masnata@unipa.it

Abstract. In the context of hybrid passive vibration control, the effectiveness of the Tuned Liquid Column Damper (TLCD) for seismic protection of base-isolated (BI) systems has been demonstrated both numerically and experimentally. In contrast to the previous studies on TLCDs, the present study explores the possibility of equipping a BI system with a sliding model of TLCD (STLCD), until now introduced only for the suppression of wind-induced vibrations of fixed-base structures. Specifically, the proposed STLCD consists of a U-shaped tank partially filled with water, mounted on a roller support and connected to the BI system via a spring-dashpot system. The validity of the introduced mathematical model is assessed by means of an extensive shaking table testing campaign at the Laboratory of Experimental Dynamics at the University of Palermo, Italy. For the experimental tests, a small-scale model of a single-degree-of-freedom (SDOF) BI structure with the STLCD is constructed, and the effectiveness of the proposed combined control strategy is experimentally evaluated. Finally, comparisons with traditional TLCDs and TMDs are made and the control efficiency is discussed with emphasis on the reduction of the accelerations of the BI system.

1. Introduction

As widely recognized, the effectiveness of seismic base isolation (BI) as structural protection technique against the destructive effects of earthquakes relies upon its ability to mitigate the impact of seismic-induced vibrations through the use of isolator devices [1]. These devices, generally installed between the foundation and the superstructure, are designed to have both low lateral and high vertical stiffness to resist large deformations without failing under the structural loads. The BI system acts like a low-pass filter on the earthquake ground motion, allowing the first natural frequency of the structure to be shifted out of the potential energy content frequency range, resulting in reduced responses of the superstructure. Nevertheless, BI structures may experience high displacements and accelerations at the base during unfavorable seismic excitations [2]. To address this issue, many studies have considered the application of the so-called hybrid control strategies [3], based on the combination of BI systems with additional energy dissipation mechanisms properly tuned to the natural frequency of the BI system. The concept arose from the observation that the response of well-isolated systems is dominated by the first-modal contribution, and that the most common absorbers, such as the Tuned Mass Dampers (TMDs) and Tuned Liquid Column Dampers (TLCDs) passive control devices, are particularly effective at reducing this fundamental vibration mode. Unlike controlled fixed-base structures, the additional device is attached directly to the base to avoid stresses in the main structure due to the added weight. The first passive control device studied in conjunction with the BI system was the TMD [4,5], which is a secondary mass, usually in steel or concrete, attached to the structure via a spring and a damper.

Although experimental tests and real-world applications confirm the effectiveness of TMDs [6,7], interest in TLCDs has increased in the last decade due to their advantageous features. TLCDs contain a liquid mass that can oscillate inside a U-shaped tank and dissipate structural vibrations by using gravity as the restoring force and both the viscous interaction and head loss between the liquid and the container as the damping force [8]. Notably, liquid dampers possess advantages over other damping devices such as lower installation costs and less maintenance. Additionally, when water is used as the liquid, it can be utilized for water supply and firefighting. Furthermore, TLCDs are economical and flexible since they can be easily tuned to the primary structure by changing the length of the liquid column. Since the liquid column length cannot be reduced below a certain value, TLCDs are generally long-period systems used for flexible structures and are therefore particularly suitable for BI structures. In this context, Hochrainer and Ziegler [8] investigated numerically the effect of a TLCD on a BI five-story frame structure, and a straightforward procedure for a direct evaluation of the TLCD parameters was proposed to reduce the seismic response of a BI multi-degree-of-freedom frame structure [9]. Although an extensive literature supports the effectiveness of the hybrid BI & TLCD strategy, there is limited experimental evidence. The first studies to experimentally investigate the control performance of a TLCD coupled with a small-scale BI three-story model frame can be found in [10,11]. Interestingly, it was highlighted that despite the slightly nonlinear properties of the BI & TLCD system, a linear analytical model can capture the experimental behavior with sufficient accuracy. Moreover, this hybrid control strategy was shown to reduce the displacement demand of both the BI system and the complete structural system. With the aim of exploiting the beneficial properties of TLCDs, the research on TLCDs was extended to encompass different topics ranging from control performance to optimization procedures and proposals of alternative TLCD configurations to maximize the efficiency of vibration mitigation [12]. However, from an experimental point of view, all previous work on the seismic enhancement of BI systems is limited to the combination with classical fixed typologies of TLCDs.

In this context, the present paper explores the possibility of the application of a sliding version of the TLCD, herein referred to as STLCD, which is essentially a spring-damper-connected model of TLCD. The STLCD is inspired by the liquid column damper (LCD) proposed by Ghosh [13]. Although in that study the LCD was investigated for seismic vibration control of short-period fixed-base structures, an interesting feature about the tuning procedure of this device emerged. Indeed, it should be noted that the need to tune the frequency of classical TLCDs as a function of the total length of the liquid column restricts their use to a limited number of structural categories. On the other hand, when employing a TLCD endowed with a spring-dashpot system, the tuning procedure is more versatile since the spring can be used for tuning and additional damping can be achieved by the dashpot. Notably, the equations of motion of the proposed BI & STLCD system can be retrieved from the formulation of a hybrid control strategy recently introduced by the authors, which couples the BI system with a moving variant of the TLCD connected to an inerter mechanism (TLCDI) [14]. Specifically, the mathematical model of the BI & STLCD control strategy results from neglecting the inerter characteristics by assuming a value of zero for its inertance.

With this background, the dynamic behavior of the proposed STLCD connected to a BI structure via a spring-dashpot system is investigated. The reliability of the theoretical model is assessed by performing experimental tests on a small-scale BI SDOF model. After a brief introduction to principles of the combined BI & STLCD control strategy, the experimental setup and model identification both are described in detail for both single elements and the overall system. The effectiveness of the proposed combined strategy in reducing the accelerations at the isolation level is analyzed through comparisons with the BI system controlled with traditional TLCD, with TMD, and without devices when subjected to harmonic excitations.

2. BI & STLCD control strategy: mathematical formulation

Consider the single-level framed base-isolated (BI) system shown in Figure 1, where M, C and K denote the mass, damping and stiffness coefficients, with the subscripts b and s indicating the BI subsystem and the main structure, respectively.

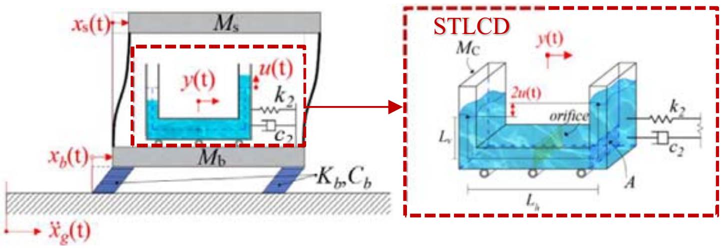

Figure 1. SDOF base-isolated STLCD-controlled structure.

The BI structure has the total mass $M_{tot} = M_b + M_s$ and is equipped with an STLCD device placed at the base, which consists of a partially liquid-filled U-shaped container connected to the BI subsystem via a spring and a damper. In the close-up figure of the STLCD device, L_v and L_h indicate the height of the liquid in the vertical portion of the L-shaped limb and the horizontal length of the device. Thus, the total length of the liquid in the container is $L = L_h + 2L_v$. The liquid tank is characterized by a constant cross-sectional area A. The total mass of the device is composed of the container mass M_c and the liquid mass $m_l = \rho AL$, where ρ is the density of the liquid. The controlled system is subjected to the horizontal ground acceleration $\ddot{x}_g(t)$ and has four degrees of freedom, i.e., the horizontal displacements $x_b(t)$ and $x_s(t)$ of the BI subsystem and the main structure, respectively, $y(t)$ and $u(t)$ indicating the horizontal displacement of the container and the vertical displacement of the liquid.

It is worth noting that the governing equations of the BI & STLCD system can be retrieved from the study on the use of the Tuned Liquid Column Damper Inerter (TLCDI) for BI structures [14] by assuming that the parameter characterizing the inerter, i.e., the inertance, is zero. Accordingly, the equations of motion of the BI & STLCD system are:

$$\begin{cases} \ddot{x}_s(t) + \ddot{x}_b(t) + 2\zeta_s\omega_s\dot{x}_s(t) + \omega_s^2 x_s(t) = -\ddot{x}_g(t) \\ \mu_b\ddot{x}_s(t) + (1+\mu_t)\ddot{x}_b(t) + \mu_t\ddot{y}(t) + \alpha\mu_l\ddot{u}(t) + 2\zeta_b\omega_b\dot{x}_b(t) + \omega_b^2 x_b(t) = -(1+\mu_t)\ddot{x}_g(t) \\ \ddot{x}_b(t) + \ddot{y}(t) + \alpha\mu_l\ddot{u}(t)/\mu_t + 2\zeta_2\omega_2\dot{y}(t) + \omega_2^2 y(t) = -\ddot{x}_g(t) \\ \alpha\ddot{x}_b(t) + \alpha\ddot{y}(t) + \ddot{u}(t) + \xi|\dot{u}(t)|\dot{u}(t)/(2L) + \omega_l^2 u(t) = -\alpha\ddot{x}_g(t) \end{cases} \tag{1}$$

where the overdot denotes the derivative with respect to time and the following symbols have been introduced: $\omega_b = \sqrt{K_b/M_{tot}}$ and $\zeta_b = C_b/(2\omega_b M_{tot})$ are the natural frequency and damping ratio of the BI subsystem, respectively; $\omega_s = \sqrt{K_s/M_s}$ and $\zeta_s = C_s/(2\omega_s M_s)$ denote the natural frequency and damping ratio of the main structure, respectively. Furthermore, $\alpha = L_h/L$ is the length ratio while $\mu_t = \mu_l + \delta$ denotes the total mass ratio of the STLCD, where $\mu_l = \rho AL/M_{tot}$ and $\delta = M_c/M_{tot}$ are the liquid and the container mass ratio, respectively. In addition, $\omega_2 = \sqrt{k_2/(\rho AL + M_c)}$ is the natural frequency of the liquid container, $\zeta_2 = c_2/[2\omega_2(\rho AL + M_c)]$ is the damping ratio, and $\omega_l = \sqrt{2g/L}$ is the natural frequency of the liquid inside the STLCD. Moreover, g is the gravity acceleration and ξ is the so-called head loss coefficient, introduced to model the hydrodynamic head losses that occur during the motion of the liquid inside the vessel [12]. It is worth mentioning that Equation (1) is characterized by a nonlinear behavior due to the presence of the nonlinear term $\xi\left|\dot{u}(t)\right|\dot{u}(t)/(2L)$ [12,15], which models the resulting turbulent eddies that cause viscous dissipation. Similarly to TLCDs, which also exhibit weakly nonlinear behavior, equivalent mechanical models can be adopted to simplify the analyses required for optimal design of the device [10,14]. In the following sections, the reliability of using an equivalent linear model is verified through experimental tests.

3. Description of the small-scale model and the experimental set-up

To study the effectiveness of the BI & STLCD combined control strategy, a small-scale model was designed (Figure 2) by assembling the following subsystems:

• A base isolated structure (Figure 2(a)) is composed of a single-story, single-bay frame system and an isolation subsystem. The first system, corresponding to the superstructure, is made up of a plexiglass plate representing the roof, 300 mm wide and with a section of 15×300 mm. Two pairs of aluminum elements with a height of 300 mm and a rectangular section of 70×0.5 mm, as well as two steel elements of 15x300x1 mm, which serve as vertical supports connecting the top plate to the BI system. The latter is made of a 15x300x300 mm plexiglass plate mounted on two parallel sliders with dimensions 60.4x40x10.6 mm. The two sliders can move on two 400 mm long rail lines supported by four steel box profiles fixed to the shake table. Moreover, the plexiglass plate of the base is connected to the shake table through two steel springs (RS components brand) arranged in parallel, each with a length of 135 mm, a diameter of 22 mm, and a stiffness of 1.63 N/mm, both fixed to an L-shaped steel profile.

• A sliding Tuned Liquid Column Damper (Figure 2(b)) is realized using a U-shaped container with a constant rectangular cross-section mounted on a linear guide of 200mm length bolted to the base. The container is filled with water. A few drops of lubricoolant fluid were added to the water to enhance the contrast and impart a reflecting surface that allows an optical laser to analyze the reflected signal. The sliding liquid tank is connected to the base plate through two springs (length 50mm, diameter 10mm, stiffness 0.2 N/mm) arranged in parallel. The springs and the total mass of the device were chosen according to the optimal tuning described in [14]. The dashpot depicted in the mathematical model in Figure 1 was not realized, thus, the inherent damping was estimated based on the intrinsic properties of the system.

The whole BI&STLCD system (Figure 2(a)) can be easily disassembled, allowing for the investigation of each subsystem: the BI system, the fixed TLCD (Figure 2(c)), and the STLCD device (Figure 2(b)). Specifically, the fixed TLCD was tested by considering the STLCD without springs and blocking the slider movement. The experimental tests were carried out at the Laboratory of Experimental Dynamics, University of Palermo using two types of shake tables: the APS 113 ELECTRO-SEIS shaker and the Quanser Shake Table II, providing the base excitation. The APS 113 ELECTRO-SEIS shaker was employed for dynamic identification of the single devices (TLCD and STLCD), while the Quanser Shake Table II was used for the larger BI structure with and without devices. During testing, the total lateral accelerations of the bottom, the base plate, the roof, and the sliding container were recorded by two different piezo-electric accelerometer typologies: DeltaTron Accelerometers Brüel&Kjaer Type 4507-002B and PCB-Type 393B04, respectively. Moreover, an optical laser sensor of type optoNCDT 1420-500, manufactured by Micro-Epsilon Messtechnik GmbH, was attached to the TLCD to measure the vertical liquid displacement. Signal data originated from the accelerometers was acquired via a NI PXIe-1082 DAQ device, equipped with a high-performance multi-channel NI PXIe-4497 board. Finally, the entire system was controlled via an in-house developed signal processing software in the LabVIEW environment.

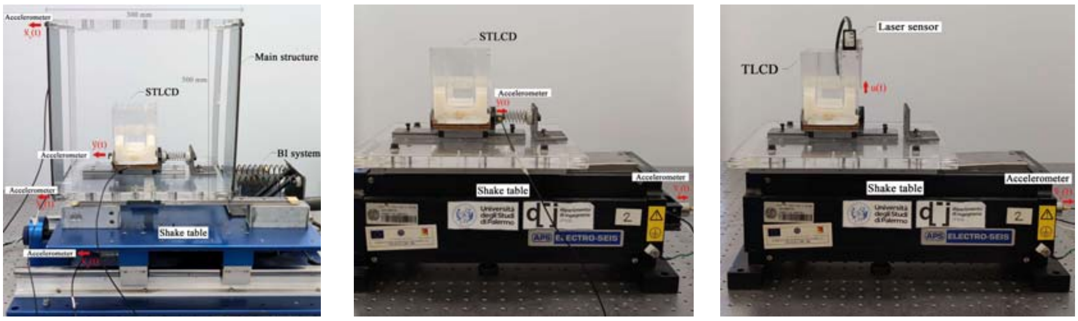

(a) *(b)* *(c)*

Figure 2. Small-scale models: (a) SDOF base-isolated STLCD-controlled structure; (b) Proposed STLCD device; (c) Traditional TLCD device.

4. System identification procedure

In order to assess the validity of the proposed mathematical model, identification procedures are applied to numerically evaluate the parameters of the hybrid-controlled BI & STLCD system so that the theoretical dynamic response of the small-scale model matches the experimental measurement data. These parameters are identified separately for each subsystem, as described in the following.

4.1. Base isolated shear frame system

The first phase of experimentation concerned the dynamic identification of the single BI small-scale model. The linear dynamic response of the system is described by using the following mathematical model [3]:

$$\begin{cases} \ddot{x}_s(t) + \ddot{x}_b(t) + 2\zeta_s\omega_s\dot{x}_s(t) + \omega_s^2 x_s(t) = -\ddot{x}_g(t) \\ \mu_b\ddot{x}_s(t) + \ddot{x}_b(t) + 2\zeta_b\omega_b\dot{x}_b(t) + \omega_b^2 x_b(t) = -\ddot{x}_g(t) \end{cases} \tag{2}$$

The frequency ω_b and the damping ratio ζ_b of the BI subsystem and the superstructure (ω_s and ζ_s) are the parameters to be identified. The mass ratio $\mu_b = M_s / M_{tot} = 0.48$ was previously determined by weighing the individual assembly parts.

For the identification of the structural parameters, the experimental model was subjected to a sine sweep signal as ground acceleration $\ddot{x}_g(t)$ ranging from 0.1 to 15 Hz in 40 seconds, which was fed by the Quanser Shake Table II. Six tests were performed and the ground acceleration (i.e., the shake table acceleration), base acceleration, and roof acceleration were recorded with the accelerometers. After the experiment, the recorded time domain-data were transferred into the frequency domain ω by application of the built-in *fft* command in MatLab to obtain the mean of the experimental frequency response functions (FRFs) of the base and top story level accelerations, taking the ground acceleration as the input signal. The objective that the experimental and analytical FRFs match yields the parameters to be identified. Specifically, the analytical FRFs in terms of the base and top story accelerations, denoted as $H_{\ddot{X}_b}(\omega)$ and $H_{\ddot{X}_s}(\omega)$, are given by Fourier transforming the system in Equation (3) as

$$H_{\ddot{X}_b}(\omega) = \frac{-\omega^4\mu_b + \omega^4 - 2i\omega^3\zeta_s\omega_s - \omega^2\omega_s^2}{\omega^4\mu_b - \left(\omega_s^2 - \omega^2 + 2i\omega\zeta_s\omega_s\right)\left(\omega_b^2 - \omega^2 + 2i\omega\zeta_b\omega_b\right)};\; H_{\ddot{X}_s}(\omega) = \frac{-\omega^4 H_{\ddot{X}_b}(\omega) + \omega^2}{\omega_s^2 - \omega^2 + 2i\omega\zeta_s\omega_s} \tag{3}$$

The nonlinear least square curve fitting method [16] (implemented with the *lsqcurvefit* built-in command in MatLab) was applied with the aim to match the two mean experimental FRFs with the corresponding theoretical ones. The identified frequencies and damping ratios are: $\omega_b = 24.64$ rad/s, $\zeta_b = 0.0316$, $\omega_s = 52.068$ rad/s and $\zeta_s = 0.0298$. As can be seen from Figure 3(a), both the FRFs

Journal of Physics: Conference Series **2647** (2024) 172005 doi:10.1088/1742-6596/2647/17/172005

computed with Equation (3) (say analytical solutions, shown by dash-dotted lines) using these parameters are in excellent agreement with the experimental ones (dotted lines). For the sake of completeness, Figure 3(b) also shows a comparison of the time history response for a harmonic sinusoidal acceleration with frequency equal to ω_b. Specifically, Figure 3(b) illustrates the base acceleration $\ddot{x}_b(t)$ relative to the ground obtained numerically by solving Equation (2) with the *ode45* built-in command in Matalb. Full agreement between numerical and experimental acceleration is also observed in the time domain.

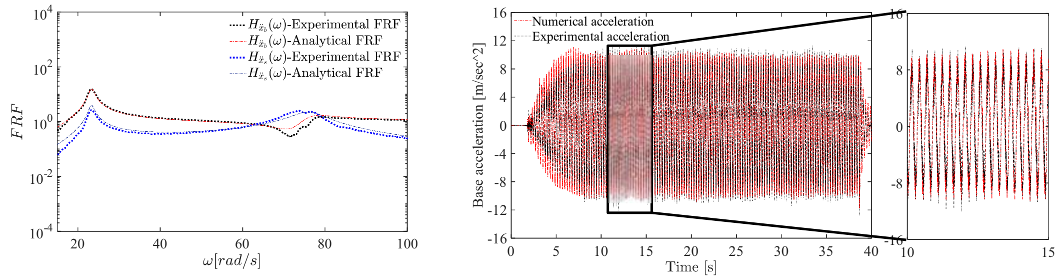

(a) *(b)*

Figure 3. Response of the BI subsystem in terms of: (a) frequency response function of the base acceleration; (b) base acceleration relative to the ground.

4.2. Sliding Tuned Liquid Column Damper

As for the procedure to determine the parameters of the STLCD device, it is worth noting that a preliminary investigation of the corresponding fixed TLCD is unavoidable. Since, as previously mentioned, the mathematical formulation of the STLCD device can be considered as a simpler version of the TLCDI device [14], deprived of the inerter mechanism, the same damping ratio of the liquid ζ_l of the conventional fixed TLCD can be considered, as already numerically demonstrated in [14]. Moreover, as proposed in [14], the frequency of the liquid can be arbitrarily chosen according to the admissible liquid quantity and dimensional/structural constraints, since the task of tuning can be assigned to the spring of the STLCD device. Specifically, a liquid mass $m_l = 168g$ is considered and the length ratio is set as $\alpha = 0.64$. Therefore, the damping ratio ζ_l and the frequency of the liquid ω_l are initially derived from the corresponding fixed TLCD. In this respect, the dynamic behavior of a base-excited TLCD is governed by the following nonlinear equation of motion [10]

$$\ddot{u}(t) + \xi\left|\dot{u}(t)\right|\dot{u}(t)/(2L) + \omega_l^2 u(t) = -\alpha\ddot{x}_g(t) \tag{4}$$

where the symbols have the same meaning as previously introduced for the STLCD. By employing the statistical linearization technique (STL) [17], as customary for weakly nonlinear TLCD systems, an equivalent linear model of the equation of motion can be adopted as follows [10]

$$\ddot{u}(t) + 2\zeta_l\omega_l\dot{u}(t) + \omega_l^2 u(t) = -\alpha\ddot{x}_g(t) \tag{5}$$

In Equation (5), only the introduced equivalent damping ratio ζ_l and the natural frequency of the liquid ω_l need to be identified in such a way that the experimental FRF of the liquid displacement matches the corresponding analytical transfer function $H_u(\omega)$ obtained by Fourier transforming Equation (5):

$$H_u(\omega) = \frac{-\alpha}{-\omega^2 + 2i\omega\zeta_l\omega_l + \omega_l^2} \tag{6}$$

In the underlying tests, the TLCD is attached directly to the APS shaker as depicted in Figure 2(c). In order to apply the SLT, the TLCD is first subjected to a band-limited white noise base excitation with a frequency range of 0.1-15 Hz. Specifically, six samples of broadband noise with a duration of 120s were generated and used as ground acceleration. Low-amplitude dynamic tests were conducted to avoid water spilling out of the TLCD container. In this manner, sloshing effects can be considered negligible since they are usually related to large-amplitude excitations. For each sample, the acceleration at the ground and the free water surface displacement were recorded through the accelerometer and the optical sensor, respectively. Based on these data, the averaged experimental FRF is computed, taking the ground acceleration as the input signal and the liquid column displacement as the output signal. Analogously to the case of the BI structure, the TLCD parameters of the mathematical model (ω_l and ζ_l) in Equation (5) are evaluated by resorting to the nonlinear least square curve fitting method. From the test results, it is found that ω_l is 14.87 rad/s and ζ_l is 0.0741. Figure 4 shows that the FRF experimentally obtained (black dotted line) sufficiently matches the analytical one (red dash-dotted line), and the recorded free water surface displacements are compared with those computed by using the linear model in Equation (5). The experimental and analytical results agree well in terms of frequency and time history responses, indicating that the linear approximation is sufficiently accurate for low excitation levels. Consequently, once the natural frequency ω_l and damping ratio ζ_l of the liquid are determined, they can be used as parameters of the liquid in the STLCD. In this manner, the remaining parameters of the STLCD, i.e., the damping ratio ζ_2 and the frequency ω_2, can similarly be identified using an equivalent linear model. The total mass and spring constant of the STLCD were set in such a way that $\omega_2 \cong 0.8-0.9\omega_b$ according to the optimal tuning procedure proposed in [14].

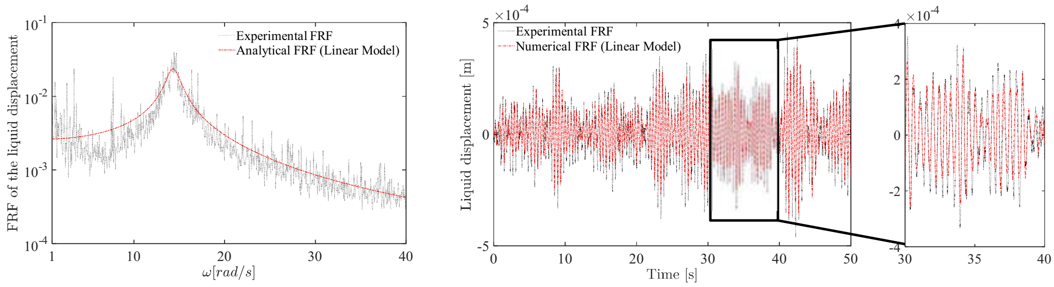

Figure 4. Response of the traditional TLCD device in terms of: (a) FRF of the liquid displacement; (b) liquid displacement.

The equations of motion for the STLCD excited at the base can be expressed as

$$\begin{cases} \ddot{y}(t)+\alpha\mu_l\ddot{u}(t)/\mu_t+2\zeta_2\omega_2\dot{y}(t)+\omega_2^2 y(t)=-\ddot{x}_g(t) \\ \alpha\ddot{y}(t)+\ddot{u}(t)+2\zeta_l\omega_l\dot{u}(t)+\omega_l^2 u(t)=-\alpha\ddot{x}_g(t) \end{cases} \tag{7}$$

The same liquid mass as the TLCD is considered for the STLCD, and taking into account a container mass equal to $M_c = 470g$, the resulting total mass ratio is $\mu_t = 0.12$ and the liquid mass ratio is $\mu_l = 0.02$. Six experimental tests were performed by exciting the STLCD by sweep sine tests in the frequency range 0.1-15 Hz, and again the averaged experimental FRFs were obtained. The STLCD parameters are determined with the nonlinear least square curve fitting method by imposing a match between the experimentally FRF of the acceleration of the STLCD container and its analytical counterpart:

$$H_{\ddot{y}}(\omega)=\frac{-\alpha^2\omega^4\mu_l-\omega^2\mu_t\left(-\omega^2+2\mathrm{i}\omega\zeta_l\omega_l+\omega_l^2\right)}{\alpha^2\omega^4\mu_l-\mu_t\left(-\omega^2+2\mathrm{i}\omega\zeta_2\omega_2+\omega_2^2\right)\left(-\omega^2+2\mathrm{i}\omega\zeta_l\omega_l+\omega_l^2\right)} \tag{8}$$

The identified damping ratio and frequency of the STLCD are: $\zeta_2 = 0.0168$ and $\omega_2 = 22$ rad/s. As can be seen in Figure 5, the experimental and numerical responses match satisfactorily in both the frequency and time domain, confirming that the approximate linear behavior of the fluid column is sufficiently accurate to model also the STLCD response. Furthermore, this approach experimentally verifies the assumption, theoretically demonstrated in [14], to use for the SLTCD the same parameters for the liquid as for the fixed TLCD.

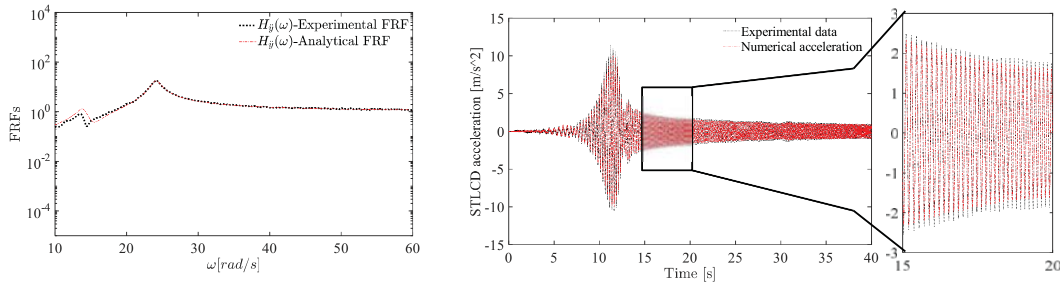

(a) *(b)*

Figure 5. Response of the STLCD device in terms of: (a) FRFs of the STLCD acceleration; (b) acceleration of the STLCD container.

5. Performance of the hybrid-controlled structure

Finally, the dynamic behavior of the hybrid-controlled system equipped with the STLCD is studied and its performance control is experimentally assessed in comparison to three types of structures: the BI structure equipped with the corresponding fixed TLCD (Figure 6(b)), the BI structure endowed with a TMD with the same STLCD mass ratio (Figure 6(c)), and the benchmark BI structure without devices, previously analyzed in Section 4.1. The TMD device was tuned according to the classical formulation proposed by Den Hartog [4] and an analogous identification procedure was applied to the TLCD and STLCD (details about the mathematical model, here omitted for brevity, can be found in [3]).

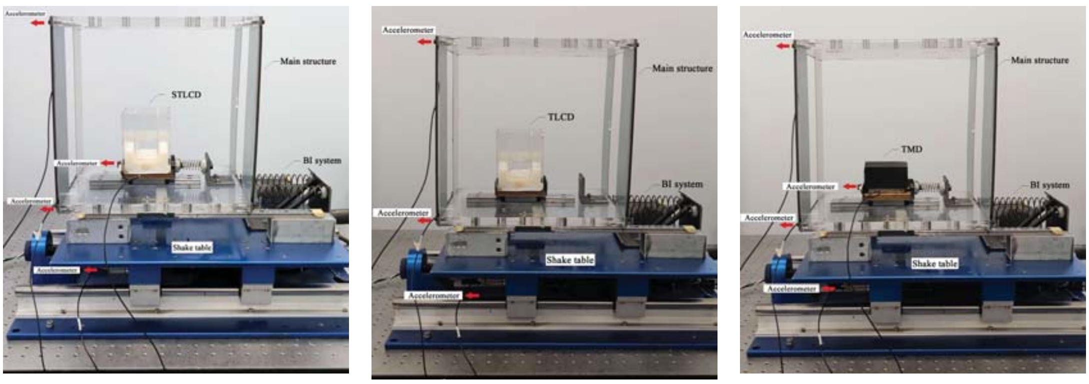

(a) *(b)* *(c)*

Figure 6. Small scale models: (a) BI&STLCD system; (b) BI&TLCD system; (c) BI&TMD system.

Specifically, since the previous results have shown that the slightly nonlinear behavior of both the TLCD and STLCD devices can be captured sufficiently accurately by a linear analytical model, the following equivalent linear equations are taken into account for the BI & STLCD system:

Journal of Physics: Conference Series **2647** (2024) 172005 doi:10.1088/1742-6596/2647/17/172005

$$\begin{cases} \ddot{x}_s(t) + \ddot{x}_b(t) + 2\zeta_s\omega_s\dot{x}_s(t) + \omega_s^2 x_s(t) = -\ddot{x}_g(t) \\ \mu_b\ddot{x}_s(t) + (1+\mu_t)\ddot{x}_b(t) + \mu_t\ddot{y}(t) + \alpha\mu_l\ddot{u}(t) + 2\zeta_b\omega_b\dot{x}_b(t) + \omega_b^2 x_b(t) = -(1+\mu_t)\ddot{x}_g(t) \\ \ddot{x}_b(t) + \ddot{y}(t) + \alpha\mu_l\ddot{u}(t)/\mu_t + 2\zeta_2\omega_2\dot{y}(t) + \omega_2^2 y(t) = -\ddot{x}_g(t) \\ \alpha\ddot{x}_b(t) + \alpha\ddot{y}(t) + \ddot{u}(t) + 2\zeta_l\omega_l\dot{u}(t) + \omega_l^2 u(t) = -\alpha\ddot{x}_g(t) \end{cases} \quad (9)$$

The previously identified parameters of the several subsystems were incorporated into the analytical model, and numerical accelerations were derived and compared with the experimental data. Figure 7(a) shows the base acceleration of the BI & STLCD system subjected to the same sinusoidal acceleration as that considered in Section 4.1 for the analysis of the BI structure in resonant conditions. The dotted black and dash-dotted red lines correspond to the experimental and numerical base accelerations relative to the ground, respectively. As can be observed, the equivalent linear mathematical model of the entire BI & STLCD system in Equation (9), described by the parameters derived from the dynamic identification of each subsystem, can be considered reliable for predicting the real behavior of the small-scale model. In a final study, the effect of the proposed hybrid control strategy on the reduction of base accelerations is compared with the cases without devices and with conventional TLCD and TMD.

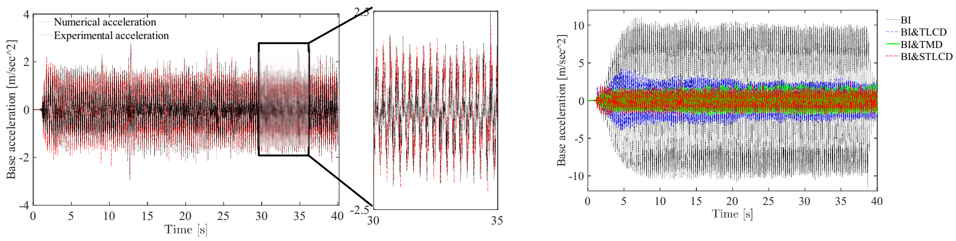

(a) *(b)*

Figure 7. Response in terms of base acceleration of (a) the BI & STLCD system (numerical versus experimental data); (b) the BI & STLCD system compared to the BI & STLCD, the BI & TLCD, and BI & TMD system.

It can be seen that the base accelerations can be significantly mitigated by up to 80% when the STLCD is attached to the BI structure (red dash-dotted line). Furthermore, it is shown that the STLCD exhibits a superior performance compared to the TLCD (blue dashed line) and is similar to the TMD (green solid line) with the same mass. However, given the versatility of the STLCD tuning procedure and the convenience of using water as additional mass can be considered an attractive device for effectively reducing accelerations at the isolation level of BI structures.

6. Conclusions

In the present paper, a novel sliding model of a Tuned Liquid Column Damper (STLCD) was presented as an alternative to conventional TLCDs for improving the effectiveness of seismic base isolation (BI) systems. Previous theoretical and experimental studies have shown that conventional TLCDs effectively protect the isolation layer from unfavorable seismic events. However, the tuning process of traditional TLCDs limits their use to a narrow range of structures, while the more versatile tuning procedure of the STLCD may broaden their application. The validity of the theoretical model of the proposed BI&STLCD hybrid control strategy was verified through small-scale shaking table experiments. In particular, the characteristic dynamic parameters of the three subsystems composing the final model (the single-story BI structure, the TLCD, and the STLCD) were identified separately and used in a comparative study to evaluate the effectiveness of the BI&STLCD system in contrast to the BI system, the BI & TLCD system, and the BI & TMD system. The results showed that the slightly nonlinear behavior of the system can be sufficiently accurately captured by a linear analytical model. Additionally, the base accelerations of the isolation layer can be reduced by up to 80% for a sinusoidal harmonic ground acceleration. The experimental tests conducted on this small-scale system show the efficacy of the BI & STLCD strategy over the conventional strategy with TLCD as a seismic protection technique. Overall, the proposed experimental study warrants further research efforts to investigate different seismic inputs, specimen sizes, and variable values (i.e., dimensions and length ratios, mass ratios, and liquid type) to ensure the validity of the results obtained.

7. Acknowledgment

Authors gratefully acknowledge the support received from the Italian Ministry of University and Research, through the PRIN 2017 funding scheme (project 2017J4EAYB 002 - Multiscale Innovative Materials and Structures "MIMS").

References

[1] Kelly JM 1990 Base-isolation: linear theory and design. *Earthquake Spectra* 6 pp 223-44.
[2] Kelly JM 1999 The role of damping in seismic isolation. *Earthquake Engineering & Structural Dynamics* 28 pp 3-20.
[3] Di Matteo A, Masnata C and Pirrotta A 2019 Hybrid passive control strategies for reducing the displacements at the base of seismic isolated structures, *Frontiers in Built Environment* 5 pp 2297-3362.
[4] Den Hartog JP 1956 *Mechanical Vibrations* New York, NY: McGraw-Hill.
[5] Yang JN and Danielians A, Li SC 1991 Aseismic hybrid control systems for building structures. *Journal of Engineering Mechanics* 117 pp 836-53.
[6] Petti L, Giannattasio, G, De Iuliis M, and Palazzo B 2010 Small scale experimental testing to verify the effectiveness of the base isolation and tuned mass dampers combined control strategy *Smart Structures and Systems* 6(1) pp 57-72.
[7] Melkumyan M 2012 New concept of a dynamic damper to restrict the displacements of seismically isolated buildings *Conference: International Conference on Advances in Materials Science and Engineering (Seoul, Korea)*.
[8] Hochrainer MJ and Ziegler F 2006 Control of tall building vibrations by sealed tuned liquid column damper *Structural Control and Health Monitoring* 13 (6) pp 980-1002.
[9] Di Matteo A, Furtmüller T, Adam C and Pirrotta A 2018 Optimal design of tuned liquid column dampers for seismic response control of base-isolated structures *Acta Mechanica* 29 pp 437-54.
[10] Furtmüller T, Di Matteo A, Adam C and Pirrotta A 2019 Base-isolated structure equipped with tuned liquid column damper: An experimental study *Mechanical Systems and Signal Processing* 116 pp 816-831.
[11] Adam C, Di Matteo A, Furtmüller T and Pirrotta A 2017 Earthquake excited base-isolated structures protected by tuned liquid column dampers: design approach and experimental verification *Procedia Engineering* 199 pp 1574-79.
[12] Konar T and Ghosh A 2022 A review on various configurations of the passive tuned liquid damper *Journal of Vibration and Control* 0(0) pp 1-36.
[13] Ghosh A and Basu B 2004 Seismic vibration control of short period structures using the liquid column damper *Engineering Structures* 26(13) pp 1905-13.
[14] Masnata C, Di Matteo A, Adam C and Pirrotta A. 2022. Efficient estimation of tuned liquid column damper inerter (TLCDI) parameters for seismic control of base-isolated structures *Computer-Aided Civil and Infrastructure Engineering* 00 pp 1-19.
[15] Bilello C., Di Paola M., Pirrotta A. 2002 Time delay induced effects on control of non-linear systems under random excitation Meccanica 37 (1-2) pp. 207 -20.
[16] Levenberg K 1944 A Method for the Solution of Certain Problems in Least-Squares *Quarterly Applied Mathematics* 2 pp 164-68.
[17] Roberts JB and Spanos PD 1990 *Random Vibration and Statistical Linearization* Chichester.